

# Rheooptical Investigation of the Transition Behavior of Polyphosphazenes<sup>†</sup>

Thomas P. Russell,<sup>‡</sup> David P. Anderson, and Richard S. Stein

Polymer Research Institute, University of Massachusetts, Amherst, Massachusetts 01003

C. Richard Desper,\* John J. Beres,<sup>§</sup> and Nathaniel S. Schneider

Army Materials and Mechanics Research Center, Watertown, Massachusetts 02172.

Received October 11, 1983

**ABSTRACT:** Wide-angle X-ray diffraction (WAXD), small-angle light, light scattering and birefringence were used to investigate the temperature dependence of the morphology of poly[bis(trifluoroethoxy)phosphazene]. Experiments conducted on solution cast films revealed a spherulitic morphology in the range 25–225 °C. Structural changes, associated with the transformation to the mesomorphic state, were found to occur in the temperature range 70–90 °C. Above the melting point, the material was isotropic by optical techniques and amorphous by WAXD. The results are discussed in terms of changes in molecular ordering.

## Introduction

Poly(organophosphazenes) of the form (RO)<sub>n</sub>PN<sub>n</sub>, where R is an alkyl or aryl group, are synthesized by substitution<sup>1–4</sup> reactions from an inorganic precursor. As a general rule, homopolymers of this type are semicrystalline at ambient temperature but undergo a first-order transition to a mesomorphic state<sup>5,6</sup> at *T*(1). The mesomorphic state is stable up to the melting temperature *T*(M), at which a true melt appears. The transitions occurring in these polymers have been characterized mechanically,<sup>1</sup> dielectrically,<sup>2</sup> thermally,<sup>3</sup> and microscopically<sup>3</sup> as well as by photographic wide-angle X-ray diffraction.<sup>3</sup>

The solid-state transformations of polyphosphazenes must be viewed in terms of the conformational behavior of the polyphosphazene molecule. On the one hand, at low concentrations the dissolved polymers exhibit a flexible coil rather than a rodlike conformation and may be characterized, as shown by Singler and Hagnauer,<sup>4</sup> by standard dilute solution techniques. On the other hand, the solid polymer shows a mesomorphic phase in which molecules are extended in one dimension over a number of chemical repeat units, which are ordered in a two-dimensional array in the plane normal to the chain direction. In this mesomorphic state the extended molecules are not held in that conformation by the close-packing interactions of the crystalline forms and show evidence<sup>7</sup> of extensive internal rotational motion. In this regard, recent work of Aharoni<sup>8</sup> has demonstrated the thermodynamic stability of an anisotropic phase, indicative of an extended molecular conformation, in concentrated polyphosphazene solutions, i.e., above 50% polymer content. This suggests that the extended conformation is stabilized by interactions between polymer chains.

Two areas of study appeared to merit further attention. First, the thermal transition behavior appears at times to be irreversible, dominated by time- and temperature-dependent annealing effects.<sup>3</sup> Under other circumstances, however, reversible behavior is observed.<sup>3</sup> A better understanding of the transition phenomenon was needed to clarify this behavior. Second, the microscopic studies revealed an intensification of the field of view between crossed polars with increased temperature, but no quan-

titative measurements were performed. In the present work, quantitative wide-angle X-ray diffraction (WAXD) measurements were conducted throughout the entire temperature range using a solid scintillation counter with slit geometry. In addition, the previous measurements were extended by carrying out small-angle light scattering (SALS) and birefringence measurements as a function of temperature.

## Experimental Section

The synthesis of the poly[bis(trifluoroethoxy)phosphazene] (I) used in this investigation has been discussed elsewhere.<sup>3</sup> Films were cast from 3% (w/v) solutions of the polyphosphazene in purified tetrahydrofuran at room temperature, with the casting volume being changed to achieve the desired thickness.

Most of the WAXD studies employed a conventional Norelco powder diffractometer with Bragg–Brentano reflection optics in order to maximize diffraction intensity, reduce counting time, and maintain angular resolution. The instrument was fitted with a cylindrical heating cell of diameter 50 mm in which a stainless steel heating stage is used to heat the sample from below. A thermocouple embedded in the specimen stage was used for temperature control, and a second thermocouple pressed against the polymer surface verified the absence of a temperature gradient. The X-ray beam entered and exited the cell through a thin nickel foil window, which served both to enclose the cell and to filter the X-radiation. Divergence and antiscatter slits with apertures of 0.25° excluded any intensity scattered by the nickel windows. Intensities were measured with a scintillation detector using pulse height analysis. A fixed counting time permitted scanning of either the sharp 1-nm line or the diffuse 0.45-nm line maximum in 15–20 min.

A Rigaku-Denki  $\theta$ – $\theta$  diffractometer was employed for data above *T*(M). In this instrument the specimen remains fixed in a horizontal plane while both the X-ray source and the detector move above the horizontal plane by equal angles  $\theta$ . The primary beam was monochromated with pyrolytic graphite, and data were recorded with a rate meter and strip chart recorder. In both instruments, a copper-anode X-ray tube operated at 40 kV and 30 mA was used.

The poly[bis(trifluoroethoxy)phosphazene] (I) was prepared by established procedures,<sup>9</sup> purified, cast from a tetrahydrofuran solution, and thoroughly dried. For WAXD experiments with cast film the specimen was bonded to the sample stage with epoxy resin. Specimens referred to as melt crystallized were bonded to the steel substrate at 260 °C [above *T*(M)] under light pressure and allowed to cool to room temperature in 30 min. A nitrogen atmosphere was maintained over the sample throughout the X-ray experiment. The specimen thickness was at least 0.2 mm and was sufficient to absorb scattered radiation from the steel substrate.

Photographic SALS was performed with a 0.5-mW Spectra Physics Model 132 He–Ne laser. Photometric data were collected with an optical multichannel analyzer (OMA) as described by Wasiak et al.<sup>10</sup> and Russell et al.<sup>11</sup> with a 2-mW Spectra Physics

<sup>†</sup> Supported in part by grants from the U.S. Army Materials and Mechanics Research Center, The Army Research Office (Durham), and the Materials Research Laboratory of the University of Massachusetts.

<sup>‡</sup> Present address: IBM Research Laboratory, San Jose, CA 95193.

<sup>§</sup> Present address: General Tire and Rubber Co., Research Division, Akron, OH 44309.

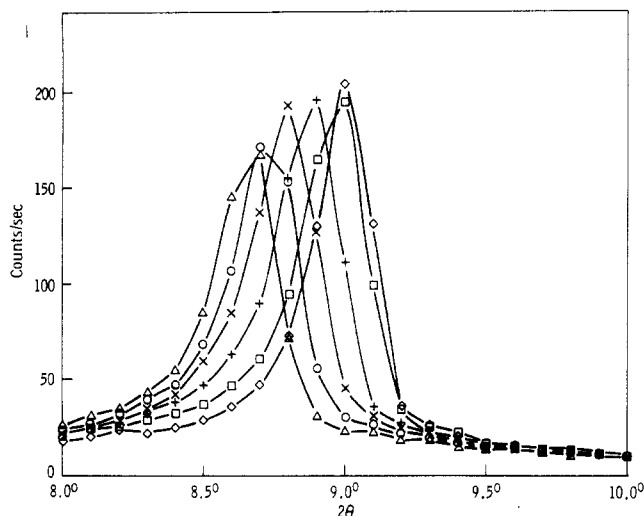


**Figure 1.** Temperature dependence of 1-nm mesomorphic line for melt-crystallized polymer: (□) 100 °C (start); (+) 135 °C; (×) 170 °C; (○) 200 °C; (Δ) 230 °C; (◊) 100 °C (end).

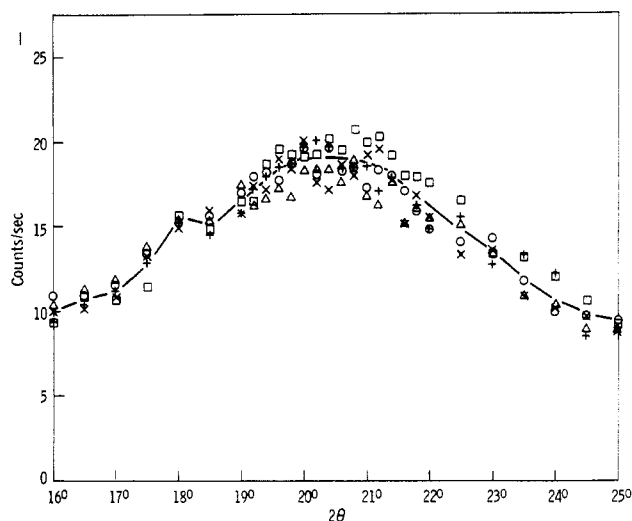


**Figure 2.** Temperature dependence of 0.45-nm maximum for melt-crystallized polymer. Symbols designate same temperatures as in Figure 1.

Model 142 He-Ne laser as a source. Birefringence measurements were performed on a Zeiss polarizing microscope equipped with a tilting compensator. Temperature control was achieved with a Mettler FP 121 hot stage.

## Results and Discussion

**WAXD.** Diffraction profiles of case and melt-crystallized film at 25 °C using the conventional diffractometer revealed diffraction peaks at 1.02, 0.93, 0.85, 0.68, 0.56, 0.44, 0.43, and 0.38 nm, in agreement with the results of Stroh.<sup>14</sup> At temperatures between  $T(1)$  and  $T(M)$ , the diffraction patterns show a strong, sharp reflection near 1 nm and a weaker, broader maximum near 0.45 nm. The sharp line has been assigned to the (100) spacing of a two-dimensional pseudohexagonal structure.<sup>12,13</sup> However, notable differences are observed between the behavior of melt-crystallized film and that of cast film. As shown in Figure 1 for melt-crystallized specimens, the 1-nm peak weakens slightly and shifts to higher  $d$  values with increasing temperature, indicating an expansion of the mesomorphic structure in the plane normal to the polymer chains. Upon return to 100 °C, the original peak position and intensity are restored, demonstrating that the structural change is reversible. The intensity maximum at 0.45 nm as shown in Figure 2 remained constant. The broad maximum arises

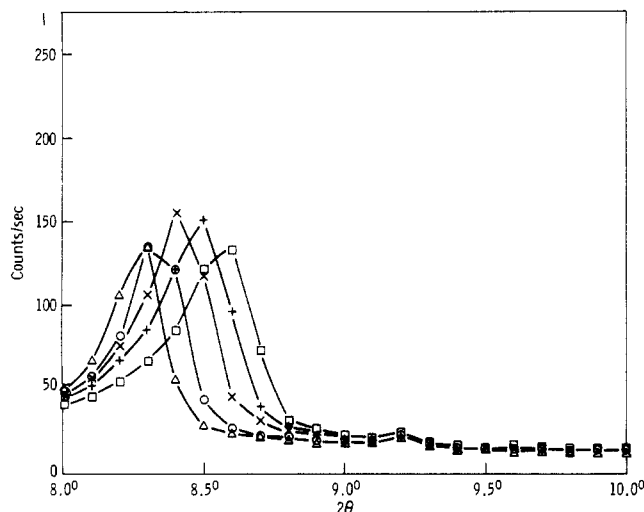


**Figure 3.** Behavior of 1-nm line for cast film, increasing temperature. Symbols designate same temperatures as in Figure 1.

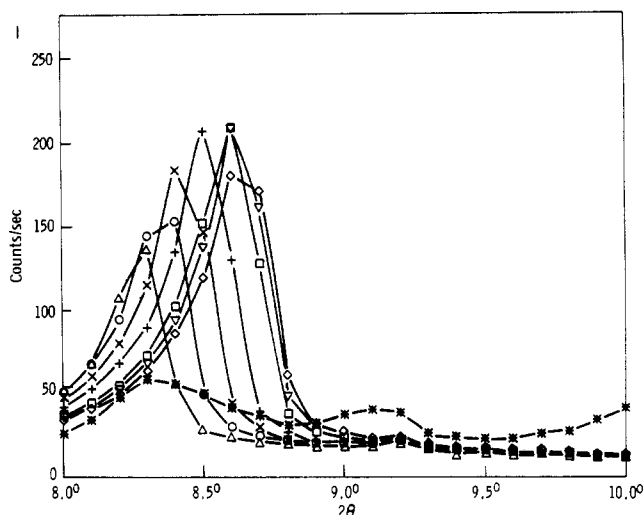


**Figure 4.** Behavior of 1-nm line for cast film, decreasing temperature: (Δ) 230 °C; (○) 200 °C; (×) 170 °C; (+) 135 °C; (□) 100 °C; (▽) 90 °C; (◊) 80 °C; (\*) 70 °C.

from interatomic correlations of intramolecular origin. Thus, while increasing temperature between  $T(1)$  and  $T(M)$  causes the mesomorphic structure to expand in two dimensions by increasing the distances between chains, the intramolecular spatial correlations undergo little change. It is recognized, of course, that the molecular structure undergoes rapid internal rotational motions, as has been shown through nuclear magnetic resonance by Alexander et al.<sup>7</sup> However, the X-ray results show that the time-averaged molecular structure undergoes little change within the mesomorphic range. The results for solution-cast films are shown in Figure 3. In contrast to the melt-crystallized specimens, an annealing effect is seen in data for the 1-nm line. As the temperature increases to 230 °C, a small increase in peak intensity is seen initially, followed by a decrease in peak intensity at higher temperatures. The latter changes parallel the reversible decrease seen at higher temperatures in the melt-crystallized sample. Upon reduction of the temperature from 230 to 100 °C, the data in Figure 4 show that the 1-nm line increases in intensity by 50%, a much greater relative increase than the reversible change of 15% observed for melt-crystallized film in this range. Thus, as temperature is either raised or lowered between  $T(1)$  and  $T(M)$ , significant irreversible effects are found in the intensities of the reflections but not in their positions. The sample was

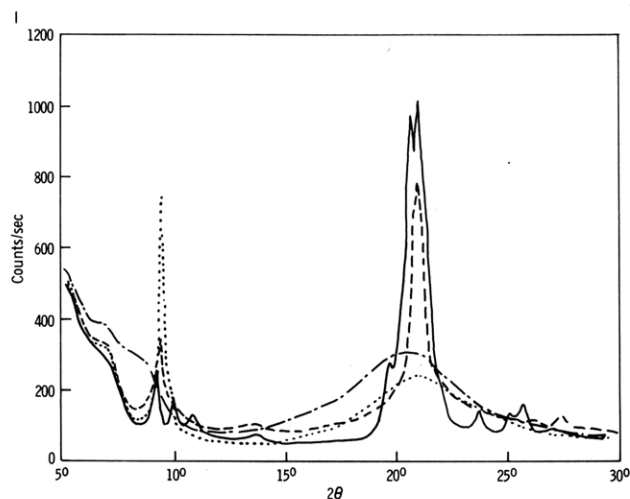


**Figure 5.** Heating experiment on the  $\theta$ - $\theta$  diffractometer, beginning with cast film: (---) 25 °C (start); (···) 101 °C; (-·-) 260 °C; (—) 24 °C (end).

held at each temperature for an average of 20 min to record the 1-nm line data, and annealing effects are seen in the WAXD intensity for both the increasing and decreasing temperature parts of the cycle. It is evident that processes that require a long time to complete are involved. It is all the more noteworthy, then, that the annealing process is rendered essentially complete<sup>3</sup> by short-term exposures above  $T(M)$  as the melt-crystallized sample is prepared from cast film.

The four diffraction patterns shown in Figure 5 were obtained with the  $\theta$ - $\theta$  diffractometer. The 1-nm line characteristic of the mesomorphic state is quite strong in the pattern at 101 °C [between  $T(1)$  and  $T(M)$ ] but disappeared in the 260 °C pattern [above  $T(M)$ , confirming that a transformation to a true melt occurs at  $T(M)$ ]. However, the 1-nm line persists, albeit at reduced intensity and in the presence of crystalline lines, at temperatures well below  $T(1)$ . The original cast film at 25 °C shows the 1-nm line near  $2\theta = 9^\circ$ , along with poorly resolved crystalline lines at  $2\theta = 13^\circ$  and  $21^\circ$ . After heating to 101 and 260 °C, followed by cooling to 24 °C, the same 1-nm line appears in Figure 5 along with a number of sharp crystalline lines. Evidently the crystallization is a slow process, and the mesomorphic phase can persist as a metastable phase well below  $T(1)$ .

Experiments with a variety of thermal treatments as shown in Figure 6 demonstrate that the crystalline and mesomorphic structures tend to coexist at ambient temperature. The crystalline material is evidenced by several sharp lines near  $2\theta = 21^\circ$  that are resolved to varying degrees after different thermal histories, while the sharp line at  $d = 1.02$  nm indicates the presence of mesomorphic material. Stroth<sup>14</sup> reports the 1.02-nm line as a crystalline line but was unable to index a unit cell. The identification of this spacing with the mesomorphic structure above  $T(1)$  and its lack of correlation in intensity with the crystalline lines at  $2\theta = 21^\circ$  in Figure 6 suggest that this line arises from mesomorphic material in coexistence with the crystalline material. Attempts to quench to the mesomorphic state at 25 °C without crystallization met with no success, since this temperature is well above the glass temperature of the polymer. At the other extreme, annealing below  $T(1)$  promotes crystallization and greatly weakens the 1.02-nm line, as seen in the 70 °C pattern at the end of the heating cycle in Figure 4.

**SALS.**  $H_v$  and  $V_v$  SALS patterns are shown in Figures 7 and 8, respectively. In the  $H_v$  series of photographs all

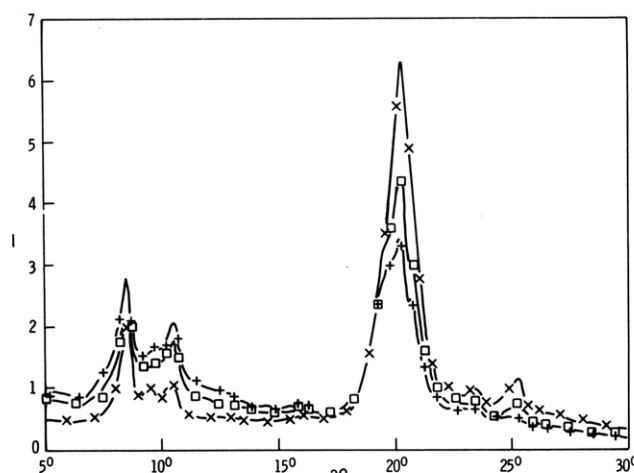


**Figure 6.** WAXD patterns of poly[bis(trifluoroethoxy)phosphazenes]: (x) melt at 260 °C, cool rapidly to 25 °C; (□) melt at 260 °C, hold 3 min at 175 °C, cool rapidly to 25 °C; (+) cast at 25 °C, hold 3 min at 175 °C, cool rapidly to 25 °C.

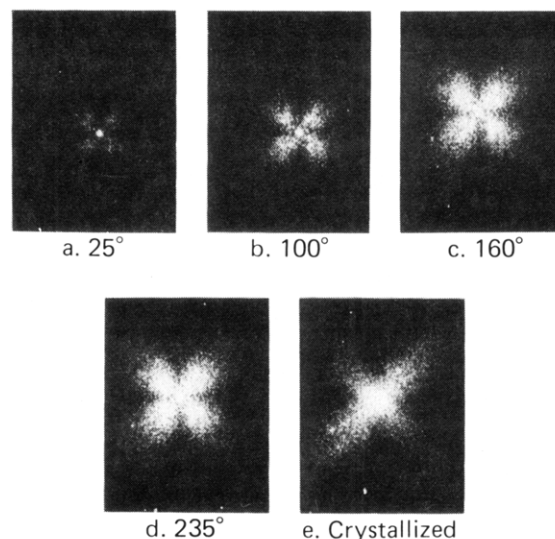


**Figure 7.** Small-angle light scattering patterns ( $H_v$  polarization) of a solution-cast film of I as a function of temperature from 25 to 235 °C. The profile in (e) was obtained after melting followed by cooling and recrystallization at 190 °C.

the parameters were kept constant, except for the temperature, to facilitate comparison. Initially, the as-cast films display a normal spherulitic scattering pattern. The actual intensity is extremely low considering the 0.25-s exposure time. The  $V_v$  scattering, on the other hand, is almost circularly symmetric. These two observations can be explained by examining the  $H_v$  and  $V_v$  scattering equations for spherulitic materials.<sup>15</sup> The intensity of  $H_v$  scattering depends upon the difference between the tangential and radial polarizabilities,  $\alpha_t$  and  $\alpha_r$ , respectively, of the spherulite. The intensity of  $V_v$  scattering depends on the differences between these two quantities and between each and the average polarizability of the material,  $\alpha_s$ . The terms in the  $V_v$  scattering equations containing  $(\alpha_t - \alpha_s)$  and  $(\alpha_r - \alpha_s)$  have no azimuthal dependence, while terms containing  $(\alpha_t - \alpha_r)$  are azimuthally dependent and thus lack circular symmetry. Since the material is volume-filled with spherulites, it can be concluded that  $(\alpha_t - \alpha_r)$  is very small and  $(\alpha_r - \alpha_s)$  and  $(\alpha_t - \alpha_s)$  dominate the  $V_v$  scattering.

As the temperature is increased above  $T(1)$ , it is evident that the spherulitic morphology is retained and that the  $H_v$  intensity increases by at least a factor of 5 before  $T_m$

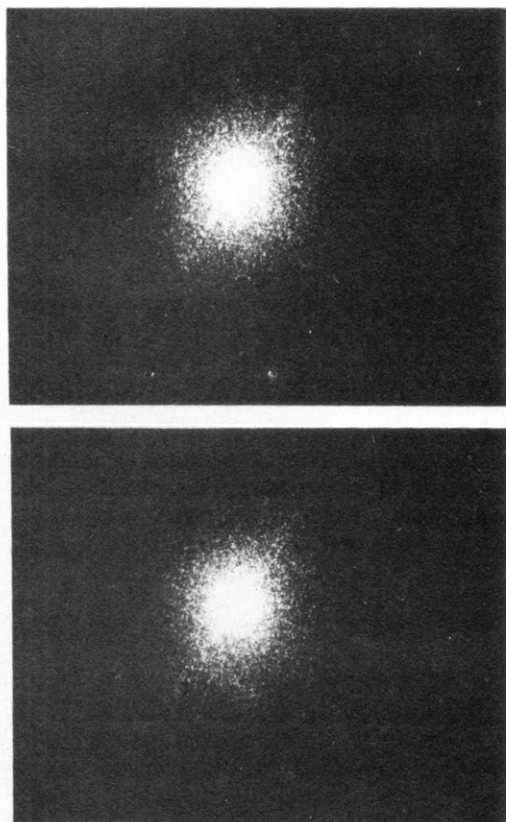


Figure 8. Small-angle light scattering patterns ( $V_v$  polarization) for a solution-cast film of I (a) at 25 and (b) 250 °C.

is reached. A less pronounced increase in the  $V_v$  scattering is seen as well. Evidently the processes occurring at the local level in the mesomorphic phase are resulting in increased optical anisotropy ( $\alpha_t - \alpha_r$ ) with little effect on the longer range density fluctuations. This result, interpreted in terms of an internal field effect, is discussed in the next section.

Similar results were seen with the optical multichannel analyzer (OMA). However, the OMA allows the photographic results to be quantified. In a volume-filled spherulitic system, if the average spherulite radius remains constant as a function of temperature, then the only parameter capable of changing the  $H_v$  intensity is the anisotropy of the spherulite ( $\alpha_t - \alpha_r$ ). Therefore, if  $T(1)$  is characterized by a process increasing ( $\alpha_t - \alpha_r$ ), then the intensity at the  $H_v$  maximum should reflect the transition as the temperature is varied. As can be seen in Figure 9, an increase in the intensity appears at approximately 70–75 °C. As the temperature is increased further, there is a continued increase in the intensity until the melting point is reached, where the intensity drops to zero, indicative of an isotropic melt.

**Birefringence.** The results from SALS can easily be verified by the measurement of the birefringence. The birefringence is related to the anisotropy of the spherulite by the equation

$$\Delta_T = \sum_i \Delta_i^0 f_i \phi_i + d_f \quad (1)$$

where  $\Delta_T$  is the total birefringence (measured),  $\Delta_f$  is the form birefringence,  $\Delta_i^0$  is the intrinsic birefringence of phase  $i$  with volume fraction  $\phi_i$  and orientation function  $f_i$ . Assuming that the form birefringence is zero and that the amorphous phase is isotropic ( $f_a = 0$ ), eq 1 for a volume-filled spherulitic material becomes

$$\Delta_T = \phi_c \Delta^0 f_{c,s} = \phi_c [2\pi(n^2 + 2)/9n] (\alpha_t - \alpha_r)_{c,s} f_{c,s} \quad (2)$$

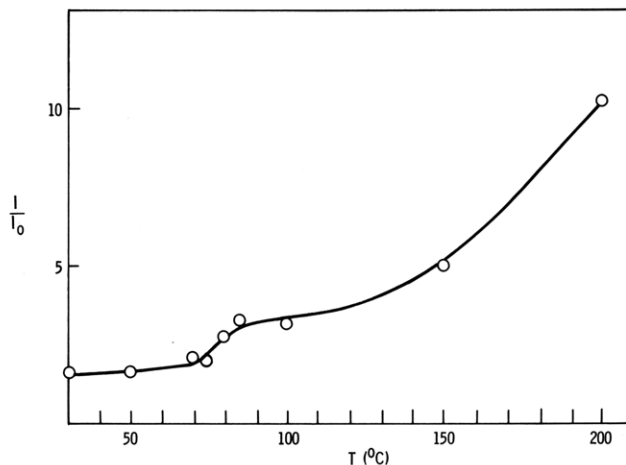


Figure 9. Maximum intensity of the  $H_v$  pattern as a function of temperature for I.

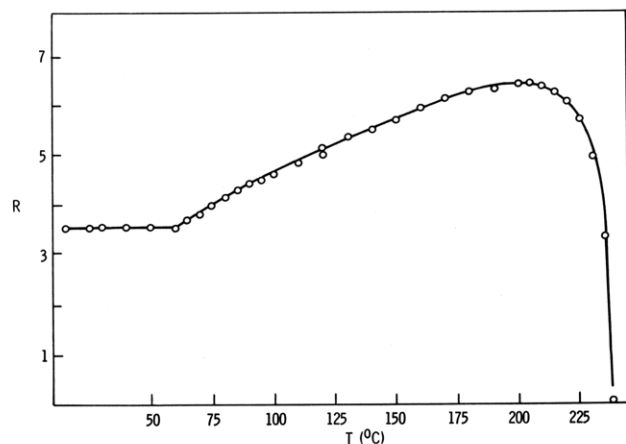


Figure 10. Retardation as a function of temperature for I after 250% elongation.

where  $n$  is the average refractive index and the subscript  $c,s$  denotes the crystalline portions of the spherulite. In this relation, birefringence has been related to anisotropy of a polarizability through the differentiated Lorenz-Lorentz equation.<sup>16</sup> Therefore, is the anisotropy of the spherulite, ( $\alpha_t - \alpha_r$ ), changes at  $T(1)$ , then  $\Delta_T$  should as well. Figure 10 shows the retardation,  $R$ , as a function of temperature from a sample that had been elongated by approximately 250%, where

$$R = \pi(2t\Delta/\lambda) \quad (3)$$

$\Delta$  is the birefringence,  $t$  is the sample thickness, and  $\lambda$  is the wavelength of the light used. The break at 60 °C is observed with a continual increase in  $R$  as a function of temperature until the melting point is reached. Upon melting, the retardation vanishes. These results parallel those obtained with SALS as would be expected if ( $\alpha_t - \alpha_r$ )<sub>s</sub> increased. At the melting point and above,  $\Delta_T = 0$ , analogous to the SALS results.

Both the birefringence and SALS results parallel the observations made in the WAXD study, suggesting that the irreversible ordering observed in the WAXD is the same as that seen by the optical methods. An important point to note is that differential scanning calorimetry does not indicate an increase in crystallinity nor a melting followed by a recrystallization during heating. This suggests a process that involves a reorganization of the chain in the spherulite, causing an increase in ( $\alpha_t - \alpha_r$ ).

The increase in optical anisotropy at the  $T(1)$  transition and above can be attributed to changes in the internal field effect, associated with the transformation from a rigid

crystal structure to a dynamically disordered mesomorphic structure. Hong, Chang, and Stein<sup>17</sup> have shown that the effect of internal field in the polyethylene crystal is to decrease its birefringence through the interaction of induced dipole moments. Such an effect should also occur in the crystals of poly[bis(trifluoroethoxy)phosphazene]. With the transformation to the mesomorphic state, the polymer chains remain extended, but the side groups undergo rapid rotational motions. The former allows the preservation of anisotropic superstructure in the absence of true crystals. The latter, it is suggested, enhances the magnitude of optical anisotropy by a reduction of the internal field effect. This interpretation is consistent with the increase in optical anisotropy at the  $T(1)$  transition (observed by polarized light microscopy<sup>3</sup> and, in the present work, by SALS and retardation of stretched film) and with X-ray and NMR data on the nature of the  $T(1)$  transition.

### Summary

A general picture of the changes involved in the thermal transition behavior of polyphosphazenes is emerging. WAXD data suggest that the mesomorphic phase coexists with the crystalline and amorphous phase. However, SAXS experiments have revealed no maximum, indicating either that the lamellae are absent or are not arranged periodically in space or that there is insufficient contrast to resolve the scattering.

For the solution-cast films at  $T(1)$  the crystalline material transforms to a mesomorphic state, but the spherulitic superstructure persists. At this point changes in the internal field effects, involved with the onset of side-group rotation, causes an increase in  $(\alpha_t - \alpha_r)$ , which is evident in the optical properties. Between  $T(1)$  and  $T(M)$  further ordering occurs in solution-cast film, either by increasing the order and/or size of mesomorphic regions or by transforming amorphous material to mesomorphic. This ordering is evidenced by increased optical anisotropy and enhanced intensity of the 1-nm WAXD line. Above  $T(M)$  all order abruptly vanishes as the molecules revert to an isotropic state.

As the melt is cooled, the trifluoroethoxy-substituted polymer does not revert to a spherulitic morphology but forms, instead, the more stable rodlike morphology. This equilibrium morphology undergoes reversible changes in the mesomorphic range and crystallizes reversibly at  $T(1) = 91.5^\circ\text{C}$ . [For cast films,  $T(1)$  is significantly lower and subject to annealing effects.] The rodlike morphology of melt-crystallized or compression-molded polymer and the reduced amorphous content account for the brittleness of these forms of polymer in contrast to the ductility of cast polymer.

Wunderlich and Grebowicz<sup>18</sup> have recently introduced the term "condis crystal", a contraction for

"conformationally disordered crystal", to describe mesophase phase of the type seen here. The basic condition for stability of a condis crystal is the existence of a series of rotational isomeric states of similar energy which do not disturb the parallel molecular arrangement. This is in accord with the basic observations and conclusions arrived at over the years about the mesomorphic phase in polyphosphazenes. In the context of the condis crystal concept of Wunderlich and Grebowicz, two important points have been explored in the present work: (a) delineation of the occurrence of both irreversible and reversible changes in properties of condis crystals, and (b) demonstration of the retention of a certain fraction of mesophase structure, which may be termed frozen condis structures, in the semicrystalline state.

**Acknowledgment.** We acknowledge the assistance of Dr. Louis J. Papa of E. I. du Pont de Nemours and Co., Inc., Wilmington, DE, who provided the  $\theta$ - $\theta$  diffractometer data.

**Registry No.** I, 28212-50-2.

### References and Notes

- (1) H. R. Allcock, R. L. Kugel, and K. J. Valan, *Inorg. Chem.*, **5**, 1709 (1966).
- (2) G. Allen, C. J. Lewis, and S. M. Todd, *Polymer*, **11**, 44 (1970).
- (3) N. S. Schneider, C. R. Desper, and R. E. Singler, *J. Appl. Polym. Sci.*, **20**, 3087 (1976).
- (4) R. E. Singler and G. L. Hagnauer, in "Organometallic Polymers", C. C. Carraher, Jr., J. C. Sheats, and C. U. Pittman, Jr., Eds. Academic Press, New York, 1978, p 257.
- (5) N. S. Schneider, C. R. Desper, and R. E. Singler, in ref 4, p 271.
- (6) N. S. Schneider, C. R. Desper, and J. J. Beres, in "Liquid Crystalline Order in Polymers", A. Blumstein, Ed., Academic Press, New York, 1978, p 299.
- (7) M. N. Alexander, C. R. Desper, P. L. Sagalyn, and N. S. Schneider, *Macromolecules*, **10**, 721 (1977).
- (8) S. M. Aharoni, *Polym. Prepr., Am. Chem. Soc., Div. Polym. Chem.*, **22** (1), 116 (1981).
- (9) R. E. Singler, N. S. Schneider, and G. L. Hagnauer, *Polym. Eng. Sci.*, **15**, 321 (1975).
- (10) A. Wasiak, D. Peiffer, and R. S. Stein, *J. Polym. Sci., Polym. Lett. Ed.*, **14**, 381 (1976).
- (11) T. P. Russell, J. T. Koberstein, R. Prud'homme, A. Misra, R. S. Stein, J. W. Parsons, and R. L. Rowell, *J. Polym. Sci., Polym. Lett. Ed.*, **16**, 1879 (1978).
- (12) C. R. Desper and N. S. Schneider, *Macromolecules*, **9**, 424 (1976).
- (13) C. R. Desper, N. S. Schneider, and E. Higgenbotham, *J. Polym. Sci., Polym. Lett. Ed.*, **15**, 457 (1977).
- (14) E. G. Stroh, Jr., Ph.D. Thesis, The Pennsylvania State University, 1972.
- (15) R. S. Stein in "Structure and Properties of Polymer Films", R. W. Lenz and R. S. Stein, Eds., Plenum, New York, 1973, pp 1-24.
- (16) J. Koberstein, T. P. Russell, and R. S. Stein, *J. Polym. Sci., Polym. Phys. Ed.*, **17**, 1719 (1979).
- (17) S. D. Hong, C. Chang, and R. S. Stein, *J. Polym. Sci., Polym. Phys. Ed.*, **13**, 1447 (1975).
- (18) B. Wunderlich and J. Grebowicz, *Polym. Prepr., Am. Chem. Soc., Div. Polym. Chem.*, **24** (2), 290 (1983); *Adv. Polym. Sci.*, in press.